Nanoscale

Accepted Manuscript

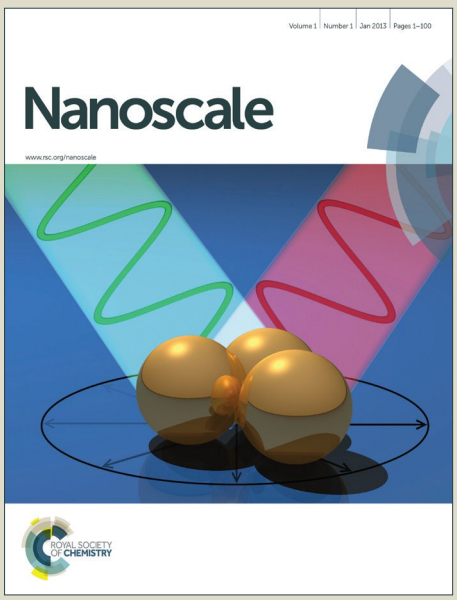

ROYAL SOCIETY OF CHEMISTRY

www.rsc.org/nanoscale

Spontaneous and specific myogenic differentiation of human mesenchymal stem cells on polyethylene glycol-linked multi-walled carbon nanotube films for skeletal muscle engineering

Chunyan Zhao[a,b], Henrik Andersen[c,d,e], Barbaros Ozyilmaz[c,d,e], Sundara Ramaprabhu[f], Giorgia Pastorin[a,b]*, Han Kiat Ho[a]*

[a]*Department of Pharmacy, Faculty of Science, National University of Singapore, Singapore 117543*

[b]*NanoCore, Engineering Block A, EA, Faculty of Engineering, National University of Singapore, Singapore 117576*

[c]*Department of Physics, National University of Singapore, Singapore 117542*

[d]*Graphene Research Center, National University of Singapore, Singapore 117546*

[e]*NUS Graduate School for Integrative Sciences and Engineering, National University of Singapore, Singapore 117456*

[f]*Department of Physics, Indian Institute of Technology Madras, Chennai, India 600036*

* Corresponding author

National University of Singapore

Pharmacy Department,

18 Science Drive 4

Singapore 117543

Fax: +65 6779 1554

Tel: +65 6516 7963

E-mail address: phahohk@nus.edu.sg (H.K. Ho), phapg@nus.edu.sg (G. Pastorin)

Abstract

This study explored the influence of polyethylene glycol-linked multi-walled carbon nanotube (PEG-CNT) films on skeletal myogenic differentiation of human mesenchymal stem cells (hMSCs). PEG-CNT films were prepared with nanoscale surface roughness, orderly arrangement of PEG-CNTs, high hydrophilicity and high mechanical strength. Notably, PEG-CNT films alone could direct the skeletal myogenic differentiation of hMSCs in the absence of myogenic induction factors. The quantitative real-time polymerase chain reaction (RT-PCR) showed that the non-induced hMSCs plated on PEG-CNT films, compared to the negative control, presented significant up-regulation of general myogenic markers including early commitment markers of myoblast differentiation protein-1 (MyoD) and desmin, as well as a late phase marker of myosin heavy chain-2 (MHC). Corresponding protein analysis by immunoblot assays corroborated these results. Skeletal muscle-specific markers, fast skeletal troponin-C (TnC) and ryanodine receptor-1 (Ryr), were also found significantly increased in the non-induced hMSCs on PEG-CNT films by RT-PCR. For these cells, the commitment to specific skeletal myoblasts was further proved by the absence of enhanced adipogenic, chondrogenic and osteogenic markers. This study elucidated that PEG-CNT films supported a dedicated differentiation of hMSCs into a skeletal myogenic lineage and can work as a promising material towards skeletal muscle injury repair.

Keywords: tissue engineering, mesenchymal stem cells, polyethylene glycol linked multi-walled carbon nanotubes, myogenic differentiation, skeletal muscle

Introduction

Skeletal muscle abnormalities can arise from a multitude of conditions like developmental anomalies, trauma, rhabdomyolysis of skeletal muscle, muscular dystrophy, diabetic tissue damage, irradiative injuries and physical injuries.[1-3] As skeletal muscle tissues show limited regeneration capacity, these conditions, coupled with substantive surgical ablations, often result in permanent damage and loss of physical mobility.[4] Consequently, much effort towards development of stem cell-based therapies was made for skeletal muscle engineering.

In tissue engineering, human mesenchymal stem cells (hMSCs) have attracted much attention due to their wide range of sources, capabilities of self-renewal in an undifferentiated state for prolonged time and multi-lineage differentiation upon proper stimuli.[5] Under appropriate conditions, mainly *via* biochemical inducers, hMSCs can differentiate into osteocytes, chondrocytes, adipocytes, myocytes and even transdifferentiate into hepatocytes, cardiomyocytes, neurons,[6] which envisage versatile applications of hMSCs. Hence, to repair and to regenerate skeletal muscle tissue, hMSCs were investigated in this study. A simple way to induce skeletal myogenesis of hMSCs was to culture hMSCs in myogenic medium supplemented with chemical inducers such as dexamethasone, hydrocortisone[1, 7] and 5-azacytidine.[8, 9] However, most chemical differentiation inducers are controversial exogenous agents with potential to cause unexpected effects to the differentiation of hMSCs. In one study, Merrison *et al.* reported that collagen substrates and medium supplemented with multiple growth factors increased the expression of skeletal muscle markers in hMSCs as demonstrated by quantitative real-time polymerase chain reaction (RT-PCR).[10] Unfortunately, the immunostaining revealed no change in expression of muscle-related proteins including desmin, myoblast differentiation protein (MyoD), myogenic factor-5 (Myf5) in hMSCs, indicating that these conditions only partially stimulated myogenic differentiation pathways. Alternatively, the use of conditioned media prepared from primary muscle precursor cell culturing media has been shown to improve the efficiency of skeletal myogenic differentiation of MSCs from human and mouse.[9, 11] However, such method requires invasive harvesting of primary skeletal muscle cells, which is hard to implement in clinical settings. Therefore, the potential use of hMSCs for skeletal muscle engineering awaits an efficient and minimally-invasive protocol that guides hMSCs towards prescribed skeletal myogenic differentiation in a controlled and reproducible manner.

It is generally hypothesized that a close imitation of the natural extracellular matrix (ECM), a complex nanostructure network, could provide a conducive environment to support the adhesion, migration, proliferation and differentiation of stem cells.[12, 13] Therefore, engineered nanomaterials have recently emerged as versatile candidates in producing scaffolds that resemble the ECM. Carbon nanotubes (CNTs), cylindrical tubes of rolled graphene sheets, have been at the forefront of nanotechnology and attracted tremendous attention for the development of scaffolds.[14] Because of their unique mechanical and electrical properties, CNTs have been used in skeletal muscle engineering to modulate the conductivity or the mechanical strength of scaffolds towards myotube formation.[15-18] For instance, electrospun polyurethane/CNTs scaffold was used to modulate skeletal myotube formation from murine skeletal muscle cells;[15] polycaprolactone (PCL)/oxidized CNT hydrogel was demonstrated to support the proliferation of rat skeletal muscle cells and displayed more myotube cells comparing to the CNT free hydrogel;[16] a recent study found that murine skeletal muscle cells grown on vertically aligned CNTs within methacrylated gelatin hydrogels yielded a higher number of myotubes than cells cultured on hydrogels with randomly or horizontally aligned CNTs, respectively.[17] However, the cells employed in these studies were skeletal muscle progenitor cells, which are harvested from skeletal muscle and have an inherent destiny towards myotube formation.[19] Additionally, there is no research investigating the sole influence of CNTs in skeletal muscle engineering. Therefore, it is a novel and bold idea to determine the influence of CNTs to the skeletal myogenesis of hMSCs which have multi-lineage differentiation ability. The result would subsequently guide us towards successful design of CNT based scaffolds for engineering specific skeletal muscle tissues.

Notably, pristine CNTs are extremely hydrophobic and rapidly precipitate in aqueous solutions, which contraindicate their biological applications. Polyethylene glycol (PEG) was thus used to modify CNTs in order to increase their hydrophilicity to facilitate scaffold preparation, cell adherence and growth.[20, 21] Therefore, in this study we report the preparation and comprehensive characterization of polyethylene glycol-linked multi-walled carbon nanotube (PEG-CNT) films and the role of PEG-CNT films in spontaneous skeletal myogenic differentiation of hMSCs. Central to our findings, the spontaneous skeletal myogenic differentiation of hMSCs plated on PEG-CNT films represents an unprecedented observation and opportunity to promote the regeneration of injured skeletal muscle.

Results and discussion

Preparation and characterization of PEG-CNT films

As a starting point for this study, advancement in film preparation was performed. In our former study, PEG-CNT films were prepared by spraying PEG-CNTs water suspension with an airbrush onto pre-heated cover slips.[20] Comparing to this method, the newly developed drop-drying method is more attractive because it is simple, cost-effective and scalable. Furthermore, the drop-drying method allows the control of film thickness by PEG-CNT concentration and suspension volume, thus minimizing batch-to-batch variability.

It was postulated that nanoscale surface roughness, which resembled the nano-architecture of the natural ECM, increased the opportunity for protein adsorption on scaffolds, facilitating stem cell attachment and differentiation.[22, 23] The typical helium ion microscope (HIM) top-view image showed that PEG-CNT films displayed a homogenous and smooth surface with nanoscale undulations (Fig. 1A). Moreover, the film surfaces exhibited an orderly fashion of PEG-CNTs. The atomic force microscope (AFM) scan of 1 μm^2 of surface topology substantiated the HIM results as the representative PEG-CNT film showed a small nanoscale Root Mean Square (RMS)-roughness of 75±9 nm with the waviness of PEG-CNT bundles. Comparing to this, the plain cover slip was extremely smooth and displayed surface roughness within 2 nm (Fig. 1B). The hydrophilicity of each substrate was evaluated by water contact angle as presented in Fig. 1C. The contact angle was found to be 17.0±3.1° for PEG-CNT films whereas 63.1±5.6° for cover slips, indicating that PEG-CNT films were more hydrophilic than cover slips. This regularity of PEG-CNTs (Fig. 1A) may be facilitated by hydrophilic PEG, which is linked to CNTs and wraps around the CNTs, reducing aggregation and finally favoring the ordered arrangement of PEG-CNTs into films. Additionally, the hydrophilic PEG block may provide PEG-CNTs with improved hydrophilicity (Fig. 1C) which could greatly enhance favorable cellular response including adhesion and differentiation.[24, 25]

Fig. 2A showed scanning electron microscope (SEM) images at the cross section of PEG-CNT films, which did not possess stratified layers but rather formed blended and porous films. The estimated thickness of PEG-CNT film was around 5µm. It is widely accepted that the indentation depth should not exceed 10% of the sample thickness in order to obtain a true load–depth response of the tested material when it is supported by a hard substrate (cover slips in this study).[26] It is desirable to choose a depth range around 10% of film thickness to acquire mechanical strength for thin films. Therefore, the average Young's modulus and hardness of PEG-CNT films and cover slips were reported in a depth range of 400-500 nm. The typical load–depth curves for PEG-CNT films and cover slips obtained from nanoindentation tests were illustrated in Fig. 2B and C. It revealed the average Young's modulus and hardness of PEG-CNT films to be 557.3±70.0 MPa and 26.3±3.0 MPa, respectively, indicative of high mechanical strength. Cover slips alone exhibited much higher stiffness than PEG-CNT films, with Young's modulus of 71.1±1.2 GPa and hardness of 6.8±0.1 MPa. A commonly known value for the Young's modulus of a single CNT (multi-walled) is 1 TPa,[27, 28] with a large variation from 0.40 to 4.15 TPa as reported by Treacy *et al.*.[29] However, this was reported for the measurement in an axial direction. The PEG-CNTs in film was observed in a radial direction in this study (Fig. 1A and B). Previous studies of Young's modulus of single CNT in the radial direction showed much lower values, between 0.3 to 4 GPa.[30] In our case of PEG-CNT films, the Young's modulus correlated with that of single CNT in the radial direction, further indicating the horizontal alignment of PEG-CNTs. Furthermore, since the PEG-CNT films are composed of a network of PEG-CNTs, the mechanical strength of the film might have been influenced by the weak inter-tube contacts such as Van Der Waals and electrostatic interactions.[31]

Viability of non-induced and myogenically-induced hMSCs

For cell culture experiments, we examined the possibility of alternative controls such as PEG-only substrates and oxidized CNT films besides uncoated cover slips. However, PEG-only matrix was deemed unsuitable since (I) the amount of PEG complexed in PEG-CNTs was very low (0.8%, mol/mol, PEG/CNTs) and such a control would be vastly different from PEG-CNTs to accurately represent the PEG effect in PEG-CNTs;[20] (II) PEG alone, being highly water soluble, would instantaneously dissolve in culture medium; (III) It was reported that PEG alone typically exhibit minimal or no intrinsic biological activity in tissue engineering, because of the lack of mechanical support and non-adhesive nature of PEG chains which cannot significantly absorb proteins or cells. [20, 32, 33] On the other hand, oxidized CNT films have been excluded from cell culture due to their instability and rapid breaking during cell culturing, which is in accordance with our previous report.[20] For these reasons, a cover slip-only control was the next best control, without having to introduce any other extraneous factors that could confound such comparison.

The cell viability at day 1, 7, 14 and 21 was evaluated by a fluorescent live/dead viability/cytotoxicity kit with calcein-AM and EthD-1. The EthD-1 reading for dead cells was minimal in every sample, which was congruent with the lack of cell death based on fluorescent live/dead staining (Fig. S1 in supplementary data). Therefore, only the reading of calcein-AM, which symbolizes viable cells, was taken in account for the calculation of cell viability. Fig. 3 showed that non-induced hMSCs on cover slips proliferated rapidly after 7 days of incubation and obtained cell viability of 224.5 ± 8.3% as compared to day 1. The cell viability reached a plateau of 248.7 ± 23.5% at day 14 and decreased marginally to 207.1 ± 7.9% at day 21. The myogenic induction decreased hMSC viability to 221.6 ± 17.1% at day 14 and 163.4 ± 5.8% at day 21. Likewise, PEG-CNT films adequately supported hMSC attachment and maintained cell viability over 21 days of incubation although cell proliferated slowly (Fig. 3). The cell viability on PEG-CNT films gradually increased to 116.5 ± 5.7% at day 7, 131.7 ± 8.8% at day 14 and 129.0 ± 4.9% at day 21 for non-induced hMSCs. With myogenic induction, the cell viability values decreased to 111.8 ± 9.8% at day 14 and 121.4 ± 6.9% at day 21. Two-way ANOVA was used to investigate the influence of substrate and induction to the cell viability. Both PEG-CNT films

and myogenic induction exerted significant effects to the reduced cell viability at day 14 and day 21 (Fig. 3). Cell proliferation and differentiation are generally alternative processes that affect stem cell phenotype. As stem cells differentiate, their rate of proliferation usually decreases.[34, 35] Hence, our observation of relatively lower cell viability with myogenic induction and slow cell proliferation on PEG-CNT films (Fig. 3) may be due to the myogenic differentiation of hMSCs and thus suppressed the proliferation of hMSCs. This was also confirmed by the lack of overt cell death based on fluorescent live/dead staining (Fig. S1 in supplementary data).

Myogenic differentiation of hMSCs on PEG-CNT films

hMSC feature markers

To determine if the treated hMSCs repressed the hMSC features and acquired myogenic gene markers distinctive in myogenesis, RT-PCR analysis was performed after 21 days of incubation. A discriminating phenotype of hMSCs is the presence of CD73, CD90 and CD105 surface molecules, as stated by the mesenchymal and tissue stem cell committee of the international society for cellular therapy (ISCT).[36, 37] As shown in Fig. 4, myogenic induction significantly attenuated the expression of CD73, CD90 and CD105. The suppressed hMSC-feature gene expression indicated that the myogenically-induced hMSCs were prone to differentiate. On the other hand, PEG-CNT films alone exerted significant effect to the reduction of CD90, but not to CD73 and CD105 (Fig. 4). This may be due to that the culturing time of 21 days is not long enough to detect significant changes on CD genes. It was found that CD markers (such as CD73) in human adipose-derived stem cells remained stable in long-term culture (until passage 20) with growth medium.[38] The *P*-value from two-way ANOVA of fold change for two variables of substrate and induction was illustrated in supplementary data Table S1.

Myogenic markers

Looking at the acquisition of myogenic phenotype, the expression of MyoD, desmin and myosin heavy chain-2 (MHC) was significantly upregulated by about 2-fold in hMSCs plated on PEG-CNT films as compared to the negative control (Fig. 5A). However, the myogenic differentiation of hMSCs was not influenced by myogenic induction as there was no significant difference in myogenic marker expression between non-induced and myogenically-induced groups. To evaluate if the increase in myogenic mRNA transcript levels was significant enough to drive to specific myogenic lineage protein expression, western blot analysis was carried out. Comparing to the negative control, the expression of MyoD and desmin was marginally higher in the myogenically-induced hMSCs cultured on cover slips (Fig. 5B). For MHC expression in hMSCs on cover slips, there was no difference between the non-induced and myogenically-induced hMSCs. However, MyoD, desmin and MHC were more strongly detected in the hMSCs cultured on PEG-CNT films with/without myogenic induction. In all, the western blot analysis (Fig. 5B) well confirmed the RT-PCR observations. Myogenic regulatory factors (MRFs) are the master regulators of skeletal myogenesis. As a member in MRFs, MyoD is required for the determination of skeletal myogenic lineages at the early stage.[39, 40] Desmin, a muscle-specific intermediate filament protein, also represents one of the earliest myogenic markers.[41, 42] Although it presents early in the development of myocytes, it is only expressed at low levels, and increases as the cell nears terminal differentiation. Contrary to this, MHC is expressed in myogenic precursors undergoing terminal differentiation.[7] Therefore, the unanimous increased expression of MyoD, desmin and MHC in differentiated hMSCs charted the progressive myogenic lineage development of hMSCs by both RT-PCR and western blot studies.

Between the two variables, only PEG-CNT film was responsible for the significant up-regulation of fast skeletal troponin C (TnC) and ryanodine receptor 1 (Ryr) (Fig. 5C). TnC is expressed exclusively in skeletal muscle and Ryr is primarily expressed in skeletal muscle.[43] Therefore, up-regulated TnC and Ryr expression in the differentiated hMSCs indicated that the hMSC-derived myoblasts may be committed towards development as a skeletal muscle cell (SKMC). Overall, there was no myogenic differentiation of hMSCs on cover slips and the myogenic induction could not improve the myogenesis of hMSCs on PEG-CNT films. The highlight of our experimental outcomes is the observation that the expression of myogenic and SKMC-specific markers significantly increased by the presence of PEG-CNT films while myogenic induction alone failed to do so (Fig. 5). This suggests that PEG-CNT films alone, without the presence of myogenic inducers like dexamethasone and hydrocortisone, could trigger the myogenesis of hMSCs (both at the transcript and protein expression levels). This is a great achievement because myogenesis was reportedly difficult to be induced in hMSCs.[44] Additionally, there is no consensus achieved so far for the optimal skeletal myogenic medium of hMSCs.[9] Therefore, dexamethasone and hydrocortisone were chosen as myogenic inducers in this study because of the simplicity, cheap price and wide usage.[1, 7] However, there is no well recognized way of controlling the optimal concentrations of these inducers for efficient differentiation with reduced or no side effects. Hence, a more important advantage of spontaneous myogenesis on PEG-CNT films is the removal of potentially noxious dexamethasone and hydrocortisone in the induction protocol.

Non-myogenic markers

Since the hMSCs can differentiate into various lineages beyond myocytes, markers for adipogenic, chondrogenic and osteogenic lineages were also investigated to assess whether this preferential myogenic differentiation of hMSCs was specific. In terms of osteogenesis (Fig. 6A), comparing to the negative control, significant decrease of collagen type I (Col-I) expression was observed in PEG-CNT film groups, whereas myogenic induction did not change this expression. For osteocalcin (OCN) expression, there was no significant impact exerted by either substrate or induction. In addition, PEG-CNT films significantly up-regulated osteopontin (OPN) levels in hMSCs while myogenic induction significantly suppressed OPN expression. On the contrary, a

significant suppression of alkaline phosphatase (ALP) was observed in PEG-CNT film groups, whereas a significant up-regulation of ALP was seen with myogenic induction. In terms of chondrogenesis (Fig. 6B), results from a two-way ANOVA showed that PEG-CNT film, myogenic induction and their interaction played roles in the significant down-regulation of SRY (sex determining region Y)-box 9 (Sox9) compared to the negative control. PEG-CNT films also exerted significant influence on the reduced aggrecan expression, whereas no significant difference was found between non-induced and myogenically-induced hMSCs. Within all treated groups, the hMSCs expressed similar levels of collagen type II (Col-II) to the negative control group without any statistically significant difference. Finally for adipogenesis (Fig. 6C), both PEG-CNT film and myogenic induction had significant influence to the decreased adipocyte protein 2 (AP2) expression in treated hMSCs compared to the negative control group. Furthermore, there was no significant difference between any two groups in adiponectin expression. Moreover, two-way ANOVA proved significant effects of PEG-CNT film, myogenic induction and interaction between the two variables to the expression of lipoprotein lipase (LPL). Notably, myogenically-induced hMSCs significantly increased LPL levels to more than 200-fold and 40-fold on cover slips and PEG-CNT films, respectively, whereas non-induced hMSCs on PEG-CNT films decreased LPL expression compared to the negative control.

To summarize (Table S1 in supplementary data), PEG-CNT films contributed to the significant up-regulation of myogenic markers of MyoD, desmin, MHC, TnC, Ryr and osteogenic marker of OPN, as well as significant down-regulation of hMSC-feature marker of CD90, osteogenic markers of Col-I and ALP, chondrogenic markers of Sox9 and aggrecan, and adipogenic markers of AP2 and LPL. Overall, PEG-CNT films coaxed hMSCs towards the phenotype of SKMCs in terms of non-enhancement or significant decrease of adipogenic, chondrogenic and osteogenic markers, as well as significant up-regulation of OPN (Fig. S2 in supplementary data). Although myogenic induction resulted in non-enhancement or significant decrease of most adipogenic, chondrogenic and osteogenic markers, it significantly increased levels of ALP and resulted in suprisingly high expression of LPL in comparison with the negative control (Fig. 6A and C). Hence, this study confirmed the possibility of removing myogenic inducers while still achieving the selectivity of skeletal myogenesis of hMSCs plated on PEG-CNT films alone. In short, the spontaneous myogenesis of hMSCs on PEG-CNT films may be a promising technique for skeletal muscle engineering.

In another study by our group, graphene (a flat instead of cylindrical material with identical molecular construct with CNTs), when coated as a matrix, alone cannot trigger the myogenic differentiation of hMSCs, but enhanced SKMC-specific markers (un-published data). These results mean that the building block that is common between graphene and PEG-CNTs is not the only determinant for the myogenesis of hMSCs. Instead, it was postulated that the characteristics of PEG-CNT films, in terms of high hydrophilicity, orderly arrangement of PEG-CNTs with nanostructure and graphene structure in the out layer, might facilitate the skeletal myogenesis of hMSCs without myogenic induction. A thorough study will be carried out in the future to investigate the mechanism underlying the spontaneous myogenic differentiation of hMSCs on PEG-CNT films.

It has been acknowledged that hMSCs have high sensitivity to the substrate “stiffness”, which directs the commitment towards different cell lineages.[45] Softer matrices that mimic brain are neurogenic, stiffer matrices that mimic muscle are myogenic, and comparatively rigid matrices that mimic collagenous bone prove osteogenic. This may explain why hMSCs on the relatively softer PEG-CNT films (average Young’s modulus of 557.3±70.0 MPa) promoted skeletal myogenesis while the hMSCs the stiffer cover slips (average Young’s modulus of 71.1±1.2 GPa) failed to do so. It is worth mentioning that the highest up-regulation of myogenic markers in the hMSCs plated on PEG-CNT films did not exceed 4-fold, which is much lower than that in SKMCs (Fig. S2). The weak myogenesis may be the result of different rigidity between PEG-CNT films and normal muscle (Young’s modulus of 12 KPa).[46] Hence, PEG-CNT scaffolds with skeletal muscle mimicked stiffness could be a future direction for a specific and ultimate skeletal myogenesis of hMSCs.

.

Materials and methods

Preparation and characterization of PEG-CNT films

Multi-walled CNTs were prepared by chemical vapor deposition method as previously reported.[47] Transmission electron microscope (TEM, FEI, Tecnai T12, USA) characterization of the CNTs indicated that the outer diameter of CNTs was 30-40 nm with an average internal diameter of about 10 nm, and the CNT length ranged from a few hundred nm to 1 µm. A representative image was shown in supplementary Fig. S3. Pristine CNTs were oxidized by sonicating in the mixture of concentrated nitric acid and sulphuric acid (1:3, v/v) for 6 hours. PEG-CNTs were synthesized from the oxidized CNTs and PEG (MW=600, Sigma Aldrich, USA) according to the procedure reported by Zhao *et al.*.[21] The PEG-CNT films were then prepared by a drop-drying method. Briefly, PEG-CNTs were sonicated in dimethylformamide (DMF) to obtain 2 mg/ml suspensions. The suspensions were subsequently dropped onto pre-heated round cover slips maintained at 160 °C. After the evaporation of DMF, PEG-CNT films were formed and the films were kept at 160 °C for other 5 minutes to remove residual DMF. The deposited PEG-CNT amount on cover slips was around 2.8 µg/mm^2.

The PEG-CNT film surfaces were imaged by HIM (Carl Zeiss, Germany). They were then measured under AFM (Dimension FastScan, Bruker, Germany) for surface roughness characterization with bare cover slips as a control. The static contact angle measurements of PEG-CNT films and cover slips were conducted by applying a 1 µl drop of deionized water to the surface and capturing an image parallel to the image plane at high magnification (WV-CP300 Day/Night Fixed Indoor Camera, Panasonic, Japan). Analysis was carried out with ImageJ software (National Institutes of Health, USA) by fitting an ellipsis to the water droplet and measuring the angle to the substrate surface baseline. The PEG-CNT film thickness was detected by SEM (JSM-6701F, JEOL, Japan) at the cross-section of the films. Mechanical strength of PEG-CNT films and cover slips was determined by MTS Nanoindenter XP (Agilent, USA). Loading rate was fixed at constant strain rate at 0.05 s^{-1} and the holding time at maximum load was 10 s. The unloading rate was the maximum loading rate incurred during loading. Continuous stiffness measurement (CSM) method was used to measure the Young's modulus and hardness. The reported values were averaged in depth range of 400-500 nm.

Cells and culture condition

The hMSCs (Lonza, Switzerlands) were expanded at 5000 cells/cm^2 in growth medium consisting of high glucose-Dulbecco's Modified Eagles Medium (DMEM, Sigma Aldrich, USA), 10% fetal bovine serum (FBS, PAA Technologies, Austria), 1% penicillin/streptomycin (Pan Biotech, Germany), 1 mM sodium pyruvate (Gibco, USA) and 1 mM non-essential amino acid (Sigma Aldrich, USA). For all experiments, hMSCs at passage 5 were used. The hMSCs were maintained at 37°C, 5% CO_2 air atmosphere and medium was replaced twice per week. Sub-culturing was conducted when cells reached 80-90% confluence with 0.25% trypsin–EDTA (Invitrogen, USA). For myogenic induction, hMSCs were cultured up to 21 days. The hMSCs at 3000 cells/cm^2 were seeded on various substrates and maintained in growth medium for 7 days. Myogenesis was then induced by changing growth medium with myogenic medium for other 14 days. The myogenic medium consisted of growth medium supplemented with 100 nM dexamethasone (Sigma Aldrich, USA) and 50 µM hydrocortisone (Sigma Aldrich, USA).[45] For the non-induced hMSCs, growth medium was used thoroughly. We included 4 experimental groups: (1) non-induced hMSCs plated on cover slips as a negative control; (2) myogenically-induced hMSCs plated on cover slips; (3) non-induced hMSCs plated on PEG-CNT films; (4) myogenically-induced hMSCs plated on PEG-CNT films.

Cell viability

The cell viability at day 1, 7, 14 and 21 was evaluated by a fluorescent live/dead viability/cytotoxicity kit (Invitrogen, USA) according to the manufacturer's instruction. Briefly, hMSCs were seeded on a 96-black-walled, clear bottom plate. On the day of experiment, cells were gently washed with PBS three times and 100 µl PBS was left after the last wash. 100 µl reagent containing 2 µM calcein-AM and 4 µM EthD-1 was added into the wells. The samples were incubated in dark at room temperature for 45 minutes and the fluorescence was measured by a plate reader (EnSpire Multimode Plate Reader, Perkin Elmer, USA). Calcein-AM was read at an excitation wavelength of 485 nm and emission wavelength of 530 nm while EthD-1 was read at an excitation wavelength of 530 nm and emission wavelength of 645 nm. The non-induced hMSCs plated on cover slips and PEG-CNT films at day 1 were used as control and defined as 100% viability for cover slip and PEG-CNT film samples respectively. Values of cell viability were expressed as a percentage of that from the control.

Quantitative RT-PCR

At the end of 21 days of incubation, hMSCs were processed for the isolation of total RNA using RNeasy Mini Kit (Qiagen, Netherland) according to the protocol given by the manufacturer. Total RNA concentration and purity were determined (OD 260/280 within 1.9-2.1) using Nanodrop (NanoDrop-ND1000, USA). cDNA of respective sample was synthesized from RNA using SuperScript III first-strand synthesis system (Invitrogen, USA).

Quantitative RT-PCR was performed with Fast SYBR Green mater mix (Qiagen, Netherland) and primers using iCycler iQ Real Time PCR Detection System (Bio-Rad Laboratories, USA). The primers for myogenic and osteogenic markers as well as hMSC-feature genes were designed by web-based Primer 3 software (http://frodo.wi.mit.edu/) and the sequences were listed

in Table 1. The cycle thermal profile comprised an enzyme activation at 50 °C for 2 minutes, followed by an initial denaturation at 95 °C for 10 minutes, 40 cycles of 95 °C for 15 s and 60 °C for 1 minute. The primer and cycle thermal profile for adipogenic and chondrogenic markers were cited from references and the primer sequences were shown in Table 2. Expression changes of various genes were analyzed using Livak ($2^{-\Delta\Delta CT}$) method to normalize gene expression to the reference gene of GAPDH to obtain ΔCT and subsequently expressed as fold change as compared to the negative control.[48] Results represented 5 independent biological replicates.

Western blot

After 21 days of incubation, cells on the substrates were lysed with cell lysis buffer (50 mM HEPES pH 7.5, 150 mM NaCl, 1 mM EDTA, 10% Glycerol, 10% Triton X-100, 10 mM sodium pyrophosphate, 100 mM sodium fluoride, 2 mM sodium orthovanadate, 2 mM PMSF, 0.1 µg/ml aprotinin). The BCA protein assay (Thermo Scientific Pierce, USA) was performed to determine protein concentration. Equal protein lysates (~20 µg) were resolved by SDS-polyacrylamide gel and transferred to polyvinylidene difluoride (PVDF) membranes (Bio-Rad, USA) for western blot. Primary antibodies were anti-MyoD (1:1000, Abcam, UK), anti-desmin (1:500, Abcam, UK), anti-MHC (1:200, Santa-Cruz Biotechnology, USA) and anti-β-actin (1:10000, Abcam, UK). Secondary antibodies were anti-mouse and anti-rabbit horseradish peroxidase conjugated secondary antibodies (Thermo Scientific Pierce, USA) at 1:10000 dilution. Each membrane was exposed to SuperSignal West Femto chemiluminescent substrate (Thermo Scientific Pierce, USA). Protein bands were then detected with enhanced chemiluminescence by feature-SRX-101A (Konica Minolta, USA).

Statistical analysis

For cell viability and RT-PCR experiments, 5 replicates were averaged and presented as mean ± standard deviation (SD). Statistical significance was determined with SPSS. Cell viability and the fold changes of each gene in RT-PCR study were analyzed using a two-way ANOVA with substrate and induction as independent variables. The *P*-values less than 0.05 denotes statistical significance.

Conclusion

We reported the fabrication and characterization of PEG-CNT films to support the growth and spontaneous skeletal myogenic differentiation of hMSCs. The PEG-CNT films, with high stiffness, presented nanoscale topography with orderly arrangement of PEG-CNTs and superior hydrophilicity on the surface. It is interesting to find that the PEG-CNT films alone triggered skeletal myogenic differentiation of non-induced hMSCs, which was substantiated by cell viability, RT-PCR and western blot analyses. Furthermore, the absence of enhanced adipogenic, chondrogenic and osteogenic markers ruled out concurrent differentiation and indicated the PEG-CNT films helped hMSCs specifically differentiate into myoblasts. This is the first report to show that PEG-CNTs can be utilized to induce the skeletal myogenesis of hMSCs. Our findings in this study suggest that the combination of hMSCs as a cell source and PEG-CNTs as a scaffold material could represent a potential strategy for skeletal muscle repair. To further challenge the capability of PEG-CNT films in directing hMSCs' lineages, trans-differentiation of hMSCs into hepatocytes, cardiomyocytes or neurons can be investigated on PEG-CNT films in future.

Acknowledgement

This work was supported by the National University of Singapore (NUS-FRC R-148-000-129-112, R148-000-187-112 and R-148-000-164-112). Thanks to Dr Daniel Pickard group (Zhongkai Ai, Hanfang Hao, Chao Fang) and Prof Venky Venkatesan group (Kingshuk Poddar, Abhimanyu Rana and Abhijeet Patra) in Nano Core for assistance in characterizing PEG-CNT films. Thanks to Dr Rachel Ee for hMSCs, to A/Prof Yap Von Bing for statistics consultation, and to Vivien Tan for assistance in the project.

References

1. H. Egusa, M. Kobayashi, T. Matsumoto, J. Sasaki, S. Uraguchi and H. Yatani, *Tissue. Eng. Part A*, 2013, **19**, 770-782.
2. J. Ma, K. Holden, J. Zhu, H. Pan and Y. Li, *J. Biomed. Biotechnol.*, 2011, **2011**, 812135.
3. M. Kaariainen and S. Kauhanen, *J. Reconstr. Microsurg.*, 2012, **28**, 581-587.
4. S. A. Riboldi, M. Sampaolesi, P. Neuenschwander, G. Cossu and S. Mantero, *Biomaterials*, 2005, **26**, 4606-4615.
5. C. Zhao, A. Tan, G. Pastorin and H. K. Ho, *Biotechnol. Adv.*, 2013, **31**, 654-668.
6. N. K. Satija, V. K. Singh, Y. K. Verma, P. Gupta, S. Sharma, F. Afrin, M. Sharma, P. Sharma, R. P. Tripathi and G. U. Gurudutta, *J. Cell. Mol. Med.*, 2009, **13**, 4385-4402.
7. E. J. Gang, J. A. Jeong, S. H. Hong, S. H. Hwang, S. W. Kim, I. H. Yang, C. Ahn, H. Han and H. Kim, *Stem Cells*, 2004, **22**, 617-624.
8. M. N. Mohammad Hassan Heidari, Zinab Namjo, Reza Frahani, Abdolali Ebrahimi, Mojgan Bandepour, Zohreh Bahrami, *J. Basic. Appl. Sci. Res.* , 2013, **3**, 9.
9. J. Stern-Straeter, G. A. Bonaterra, S. Juritz, R. Birk, U. R. Goessler, K. Bieback, P. Bugert, J. Schultz, K. Hormann, R. Kinscherf and A. Faber, *Int. J. Mol. Med.*, 2014, **33**, 160-170.
10. G. D. Merrison AFA, Scolding NJ, *J. Cell. Sci. Ther.*, 2012, **S4:001**.
11. A. D. Bajek, Tomasz; Joachimiak, Romana; Spoz, Zaneta; Gagat, Maciej; Bodnar, Magdalena; Debski, Robert; Grzanka, Alina; Marszalek, Andrzej, *Current Signal Transduction Therapy*, 2012, **Volume 7**, 8.
12. D. Liang, B. S. Hsiao and B. Chu, *Adv. Drug Deliv. Rev.*, 2007, **59**, 1392-1412.
13. E. Seyedjafari, M. Soleimani, N. Ghaemi and M. N. Sarbolouki, *J. Mater. Sci. Mater. Med.*, 2011, **22**, 165-174.
14. G. Pastorin, *Carbon Nanotubes: From Bench Chemistry to Promising Biomedical Applications*, Pan Stanford publishing Pte Ltd., Singapore, 2010.
15. S. Sirivisoot and B. S. Harrison, *Int. J. Nanomedicine*, 2011, **6**, 2483-2497.
16. K. D. McKeon-Fischer, D. H. Flagg and J. W. Freeman, *J. Biomed. Mater. Res. A*, 2011, **99**, 493-499.
17. S. Ahadian, J. Ramon-Azcon, M. Estili, X. Liang, S. Ostrovidov, H. Shiku, M. Ramalingam, K. Nakajima, Y. Sakka, H. Bae, T. Matsue and A. Khademhosseini, *Sci. Rep.*, 2014, **4**, 4271.
18. J. Xu, Y. Xie, H. Zhang, Z. Ye and W. Zhang, *Colloids Surf. B Biointerfaces*, 2014, **123**, 907-915.
19. Y. Li and J. Huard, *Am. J. Pathol.*, 2002, **161**, 895-907.
20. T. R. Nayak, L. Jian, L. C. Phua, H. K. Ho, Y. Ren and G. Pastorin, *ACS Nano*, 2010, **4**, 7717-7725.
21. B. Zhao, H. Hu, A. Yu, D. Perea and R. C. Haddon, *J. Am. Chem. Soc.*, 2005, **127**, 8197-8203.
22. M. V. Jose, V. Thomas, Y. Xu, S. Bellis, E. Nyairo and D. Dean, *Macromol. Biosci.*, 2010, **10**, 433-444.
23. B. Lei, X. Chen, Y. Wang, N. Zhao, C. Du and L. Fang, *J. Biomed. Mater. Res. A*, 2010, **94**, 1091-1099.
24. J. B. a. W. Jian Yang, *Polymers for Advanced Technologies*, 2002, **13**, 220–226.
25. M. Thomas, A. Arora and D. S. Katti, *Mater. Sci. Eng. C Mater. Biol. Appl.*, 2014, **45**, 320-332.
26. C.-M. C. Yang-Tse Cheng, *Materials Science and Engineering: R: Reports*, 2004, **Issues**, 91-149.
27. M. F. Yu, O. Lourie, M. J. Dyer, K. Moloni, T. F. Kelly and R. S. Ruoff, *Science*, 2000, **287**, 637-640.
28. B. G. W. Demczyk, Y.M; Cumings, J; Hetman, M; Han, W; Zettl, A; Ritchie, R.O *Materials Science and Engineering A*, 2002, **334** 173–178.
29. M. M. Treacy, Ebbesen, T.W., Gibson, J.M., *Nature*, 1996, **38**.
30. M. F. Yu, T. Kowalewski and R. S. Ruoff, *Phys. Rev. Lett.*, 2000, **85**, 1456-1459.
31. Q. W. a. H. Moriyama, in *Carbon Nanotubes - Synthesis, Characterization, Applications*, ed. S. Yellampalli2011.

32. J. Zhu, *Biomaterials*, 2010, **31**, 4639-4656.
33. Z. J. Singh A, Ye Z, Elisseeff JH, *Adv. Funct. Mater.*, 2013, **23**, 575–582.
34. M. Olbrich, M. Rieger, S. Reinert and D. Alexander, *PLoS One*, 2012, **7**, e47176.
35. C. GM, *The Cell: A Molecular Approach. 2nd edition.* 2000.
36. E. Mariani and A. Facchini, *Curr. Pharm. Des.*, 2012, **18**, 1821-1845.
37. M. Al-Nbaheen, R. Vishnubalaji, D. Ali, A. Bouslimi, F. Al-Jassir, M. Megges, A. Prigione, J. Adjaye, M. Kassem and A. Aldahmash, *Stem Cell Rev.*, 2013, **9**, 32-43.
38. W. K. Wan Safwani, S. Makpol, S. Sathapan and K. H. Chua, *Biotechnol. Appl. Biochem.*, 2011, **58**, 261-270.
39. V. Sartorelli and G. Caretti, *Curr. Opin. Genet. Dev.*, 2005, **15**, 528-535.
40. A. Blais, M. Tsikitis, D. Acosta-Alvear, R. Sharan, Y. Kluger and B. D. Dynlacht, *Genes Dev.*, 2005, **19**, 553-569.
41. J. D. Stewart, T. L. Masi, A. E. Cumming, G. M. Molnar, B. M. Wentworth, K. Sampath, J. M. McPherson and P. C. Yaeger, *J. Cell. Physiol.*, 2003, **196**, 70-78.
42. J. P. Beier, F. F. Bitto, C. Lange, D. Klumpp, A. Arkudas, O. Bleiziffer, A. M. Boos, R. E. Horch and U. Kneser, *Cell Biol. Int.*, 2011, **35**, 397-406.
43. R. Gahlmann, R. Wade, P. Gunning and L. Kedes, *J. Mol. Biol.*, 1988, **201**, 379-391.
44. E. J. Gang, R. Darabi, D. Bosnakovski, Z. Xu, K. E. Kamm, M. Kyba and R. C. Perlingeiro, *Exp. Cell Res.*, 2009, **315**, 2624-2636.
45. A. J. Engler, S. Sen, H. L. Sweeney and D. E. Discher, *Cell*, 2006, **126**, 677-689.
46. P. M. Gilbert, K. L. Havenstrite, K. E. Magnusson, A. Sacco, N. A. Leonardi, P. Kraft, N. K. Nguyen, S. Thrun, M. P. Lutolf and H. M. Blau, *Science*, 2010, **329**, 1078-1081.
47. R. K. Jaiswal, N. Jaiswal, S. P. Bruder, G. Mbalaviele, D. R. Marshak and M. F. Pittenger, *J. Biol. Chem.*, 2000, **275**, 9645-9652.
48. T. D. Schmittgen and K. J. Livak, *Nature protocols*, 2008, **3**, 1101-1108.
49. S. Q. Liu, Q. Tian, J. L. Hedrick, J. H. Po Hui, P. L. Ee and Y. Y. Yang, *Biomaterials*, 2010, **31**, 7298-7307.
50. B. Levi, A. W. James, D. C. Wan, J. P. Glotzbach, G. W. Commons and M. T. Longaker, *Plast. Reconstr. Surg.*, 2010, **126**, 41-52.
51. I. H. AS Mohamed, AK Soad, HB Eman, KRE Omnia, *International Journal of Experimental Pharmacology*, 2014, **4**, 29-24.

Figures

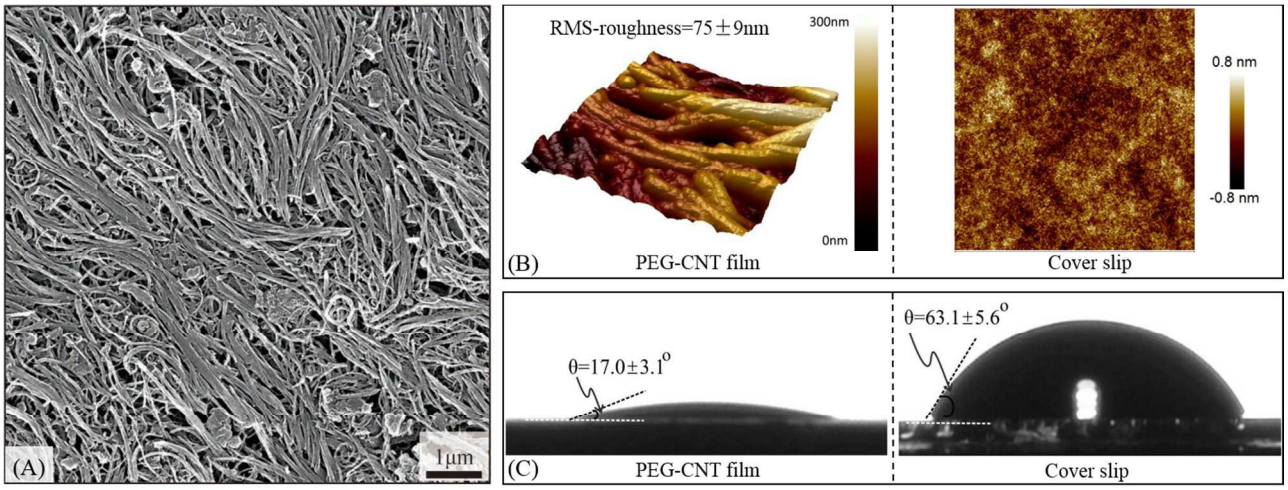

Fig. 1. (A) HIM image of the surface topography of PEG-CNT films; (B) AFM images of PEG-CNT film and cover slip surface at 1 μm^2; (C) Representative contact angles of water on a PEG-CNT film and a cover slip.

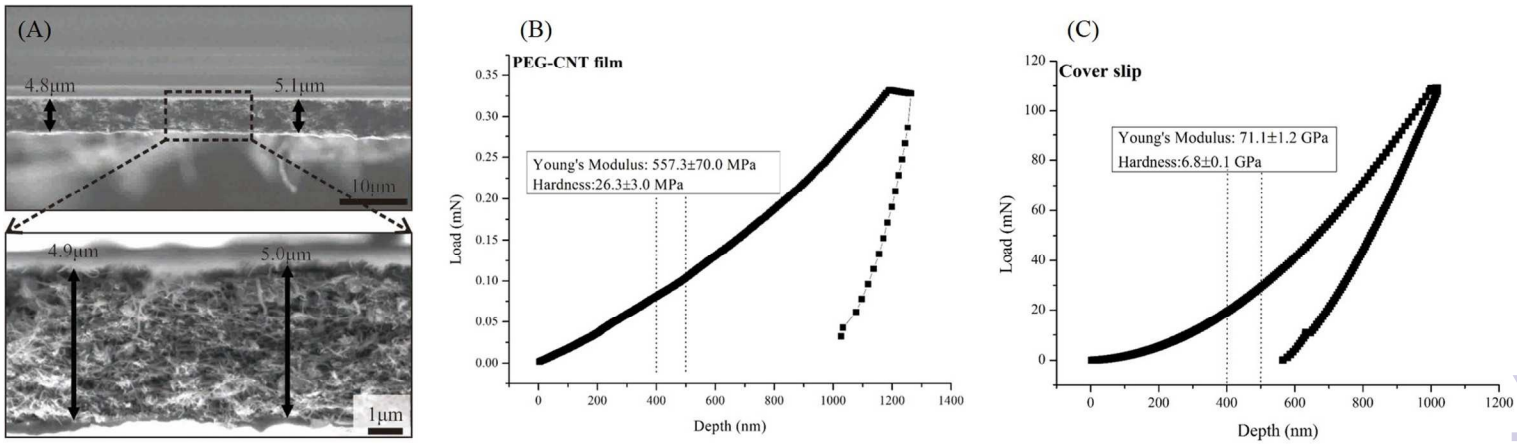

Fig. 2. (A) SEM images at the cross section of PEG-CNT films, top: 2000× magnification, bottom: zoom-in view at 10000× magnification; Representative load-depth curves of (B) PEG-CNT films and (C) cover slips by nano-indentation tests.

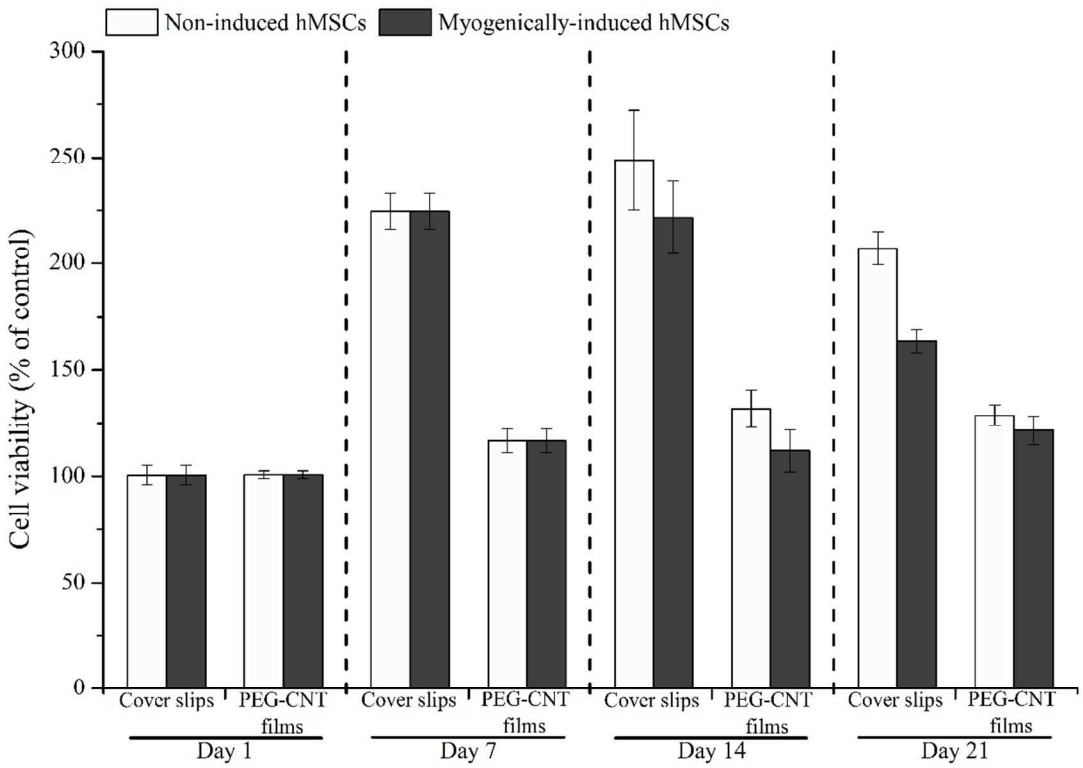

Fig. 3. Viability of hMSCs (induced to myogenic differentiation or not) on cover slips and PEG-CNT films over 21 days. Two-way ANOVA showed substrate term $P<0.001$ for day 14 and day 21, induction term $P<0.01$ for day 14 and day 21, two-way interaction term $P>0.05$ for day 14 and $P<0.001$ for day 21. The P-values less than 0.05 denotes statistical significance.

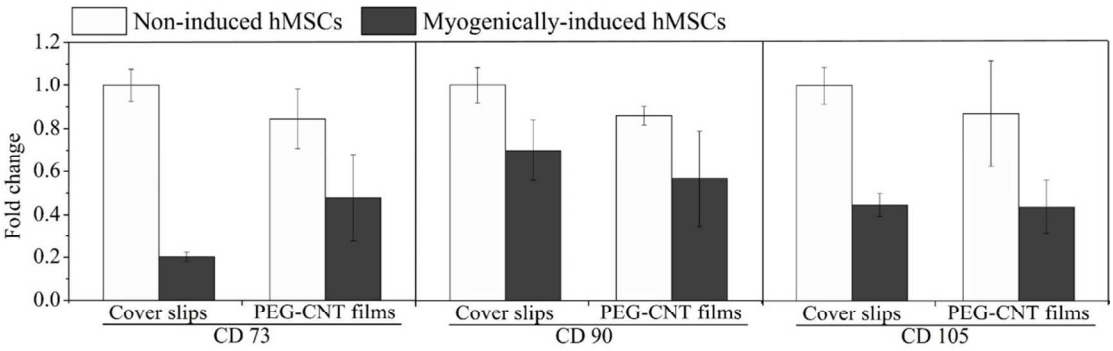

Fig. 4. Depressed hMSC-feature genes. Two-way ANOVA showed substrate term $P<0.05$ for CD90 while $P>0.05$ for CD73 and CD105, induction term $P<0.001$ for CD73, CD90 and CD105, two-way interaction term $P<0.01$ for CD73 while $P>0.05$ for CD90 and CD105. The P-values less than 0.05 denotes statistical significance.

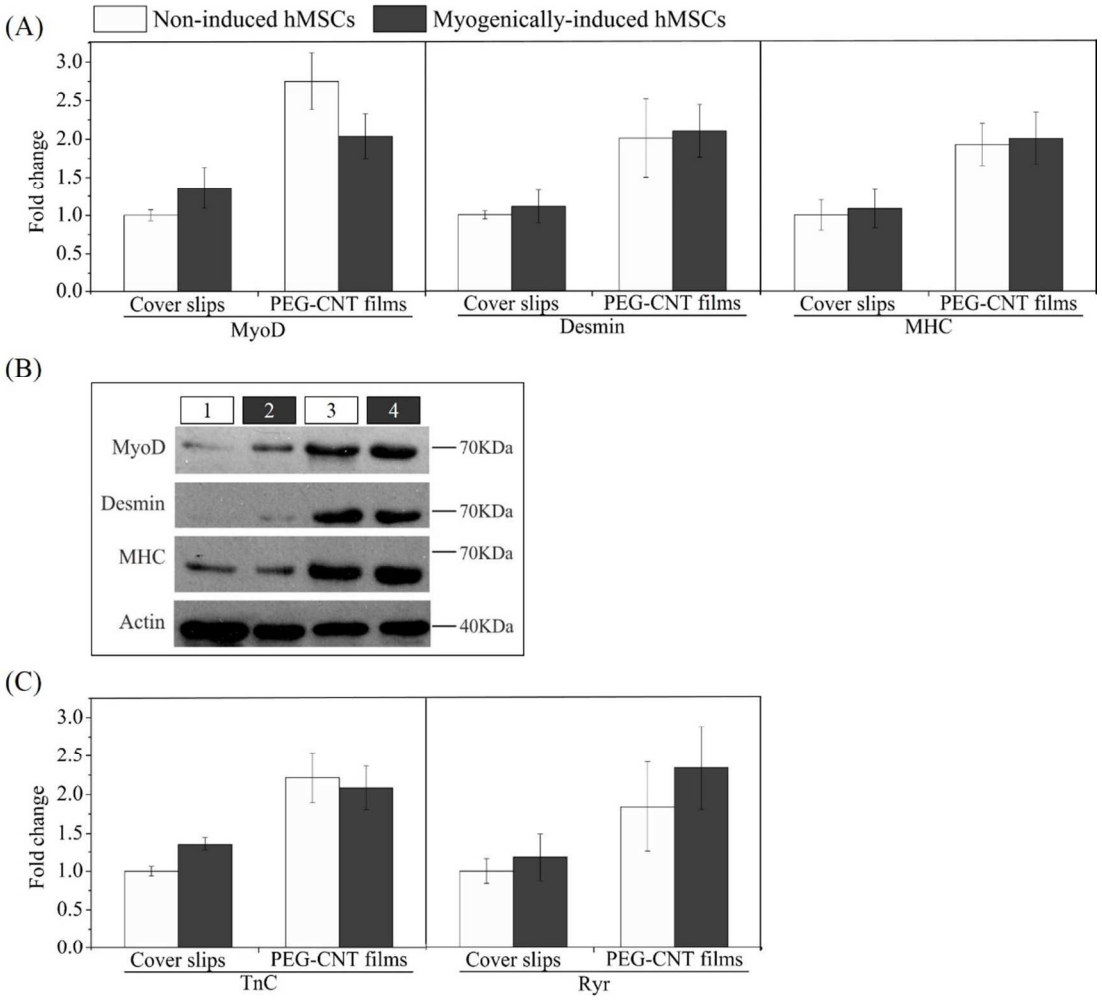

Fig. 5. (A) Up-regulation of myogenic genes in non-induced hMSCs on PEG-CNT films. Two-way ANOVA showed substrate term $P<0.001$ for MyoD, desmin and MHC, induction term $P>0.05$ for MyoD, desmin and MHC, two-way interaction term $P<0.001$ for MyoD while $P>0.05$ for desmin and MHC; (B) Western blot of myogenic proteins and actin expression in non-induced hMSCs on cover slips (lane 1), myogenically-induced hMSCs on cover slips (lane 2), non-induced hMSCs on PEG-CNT films (lane 3) and myogenically-induced hMSCs on PEG-CNTs (lane 4). Actin was used as a loading control; (C) Up-regulation of SKMC-specific genes in non-induced hMSCs on PEG-CNT films. Two-way ANOVA showed substrate term $P<0.001$ for TnC and Ryr, induction term $P>0.05$ for TnC and Ryr, two-way interaction term $P<0.05$ for TnC and $P>0.05$ for Ryr. The P-values less than 0.05 denotes statistical significance.

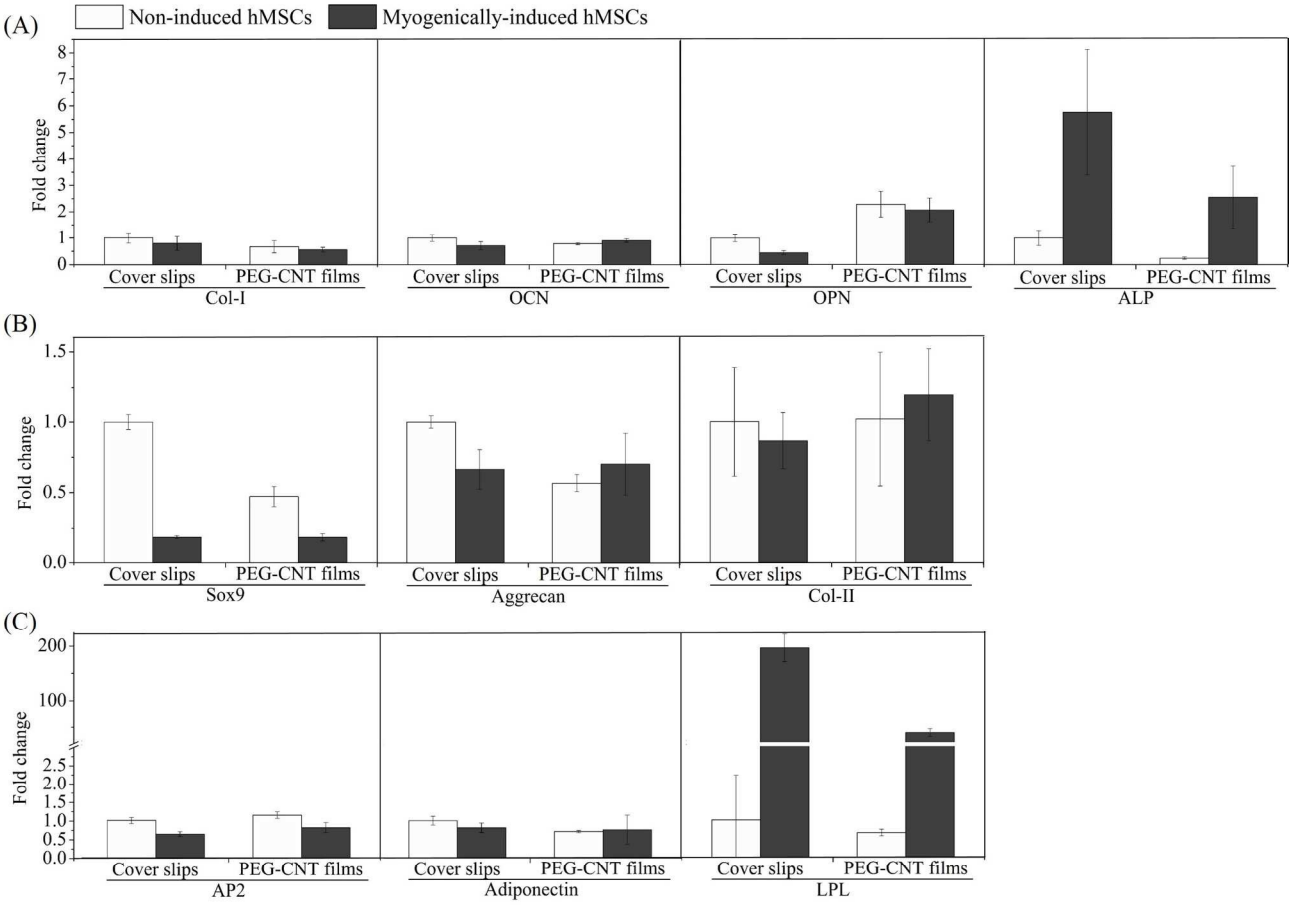

Fig. 6. (A) Osteogenic gene expression. The two-way ANOVA showed substrate term $P<0.01$, induction term $P>0.05$, two-way interaction term $P>0.05$ for Col-I; substrate term $P>0.05$, induction term $P>0.05$, two-way interaction term $P<0.01$ for OCN; substrate term $P<0.001$, induction term $P<0.05$, two-way interaction term $P>0.05$ for OPN; substrate term $P<0.01$, induction term $P<0.001$, two-way interaction term $P>0.05$ for ALP. (B) Chondrogenic gene expression. The two-way ANOVA showed substrate term $P<0.001$, induction term $P<0.001$, two-way interaction term $P<0.001$ for Sox9; substrate term $P<0.01$, induction term $P>0.05$, two-way interaction term $P<0.01$ for aggrecan; substrate term $P>0.05$, induction term $P>0.05$, two-way interaction term $P>0.05$ for Col-II. (C) Adipogenic gene expression. The two-way ANOVA showed substrate term $P<0.01$, induction term $P<0.001$, two-way interaction term $P>0.05$ for AP2; substrate term $P>0.05$, induction term $P>0.05$, two-way interaction term $P>0.05$ for adiponectin; substrate term $P<0.001$, induction term $P<0.001$, two-way interaction term $P<0.001$ for LPL. The P-values less than 0.05 denotes statistical significance.

Tables

Table 1

Sequences of primers used in RT–PCR analysis of hMSC-feature genes, myogenic and osteognenic markers.

Gene	Reference sequence number	Forward primer sequence (5'->3')	Reverse primer sequence (5'->3')	Product size (bp)
CD73	NM_001204813.1	GCC GCT TTA GAG AAT GCA AC	CTC GAC ACT TGG TGC AAA GA	234
CD90	NM_006288.3	CCC AGT GAA GAT GCA GGT TT	CAG CCT GAG AGG GTC TTG TC	183
CD105	NM_001114753.1	CAC TAG CCA GGT CTC GAA GG	CTG AGG ACC AGA AGC ACC TC	165
MyoD	NM_002478.4	CCG CTT TCC TTA ACC ACA AAT	CGG CTG TAG ATA GCA AAG TGC	98
Desmin	NM_001927.3	TCG GCT CTA AGG GCT CCT C	CGT GGT CAG AAA CTC CTG GTT	194
MHC	NM_001100112.1	GAT GGC ACA GAA GTT GCT GA	CTT CTC GTA GAC GGC TTT GG	177
TnC	NM_003279	TGG GGA CAT CAG CGT CAA G	CCA AGA ACT CCT CGA AGT CGA T	137
Ryr	NM_000540.2	TGG CTC ACC TAT GCT GCT C	GAC AGT GCG TCG TCC ATG T	101
Col-I	NM_000089.3	TCC AAA GGA GAG AGC GGT AA	CAG ATC CAG CTT CCC CAT TA	112
OCN	NM_199173.4	GAC TGT GAC GAG TTG GCT GA	CTG GAG AGG AGC AGA ACT GG	119
OPN	NM_000582.2	CAT CAC CTG TGC CAT ACC AG	GCC ACA GCA TCT GGG TAT TT	87
ALP	NM_001127501.2	CCT CCT CGG AAG ACA CTC TG	CCA CCA AAT GTG AAG ACG TG	64
GAPDH	NM_002046.4	ATG TTC GTC ATG GGT GTG AA	TGT GGT CAT GAG TCC TTC CA	144

CD73=cluster of differentiation 73, CD90=cluster of differentiation 90, CD105=cluster of differentiation 105/endoglin, MHC=myosin heavy chain 2, TnC=fast skeletal troponin C, Ryr=ryanodine receptor 1, Col-I=collagen type I, OCN=osteocalcin, OPN=osteopontin, ALP=alkaline phosphatase, GAPDH=glyceraldehyde 3-phosphate dehydrogenase

Table 2
Sequences of primers used in RT–PCR analysis of adipogenic and chondrognenic markers.

Gene	Forward primer sequence (5'->3')	Reverse primer sequence (5'->3')	Reference
Sox9	GCC TTT TTG TCC ATC CCT TTT TTC	CTC CAG GTA GCC TCC CTC ACT CC	[49]
Aggrecan	CAC GGC TTC TGG AGA CAG GAC TG	TGT TGG GGA GGT GGC TGT TTC G	[49]
Col-II	ACC TCA CGC CTC CCC ATC ATT G	ACA TCA GGT CAG GTC AGC CAT TCA G	[49]
AP2	CCA GGG ACT TTG GGT ACG TG	GGT TGA GAA ATT CAG CTA CTG CT	[50]
Adiponectin	TCC TGC CAG TAA CAG GGA AG	GGT TGG CGA TTA CCC GTT TG	[51]
LPL	TCA TTC CCG GAG TAG CAG AGT	GGC CAC AAG TTT TGG CAC C	[50]

Sox9=SRY (sex determining region Y)-box 9, Col-II=collagen type II, AP2=adipocyte protein 2, LPL=lipoprotein lipase